Hyperfine Interactions (2022) 243:5
https://doi.org/10.1007/s10751-021-01750-6

The temperature dependence of nuclear resonant X-Ray spectra of magnetic iron and cementite

L. Mauger[1] · S. H. Lohaus[2] · B. Fultz[2]

Accepted: 21 October 2021Published online: 30 December 2021

Abstract

From low temperatures through the Curie temperatures, the phonon density of states (DOS) was measured for bcc ^{57}Fe, and the partial phonon DOS was measured for cementite, $^{57}Fe_3C$, by nuclear resonant inelastic x-ray scattering (NRIXS). Nuclear forward scattering (NFS) was used to determine the state of magnetization of $^{57}Fe_3C$. The changes in phonon DOS with magnetization were assessed, and a linear relationship was found between the temperature dependences of the magnetization and the non-quasiharmonic shifts of phonon frequencies. Following the quasiharmonic approximation (QHA) for non-harmonic phonons, a magnetic quasiharmonic theory is developed to account for how phonon frequencies are altered by changes in magnetization. The formalism explains well the discrepancy between the free energy measurements and predictions of the QHA for both bcc iron and cementite. The physical origin of the magnetic Grüneisen parameters remains a challenge.

Keywords Phonons · Magnetism · Nuclear resonant scattering

These authors contributed equally to this work.

This article is part of the Topical Collection on *Proceedings of the International Conference on the Applications of the Mössbauer Effect (ICAME 2021), 5-10 September 2021, Brasov, Romania*
Edited by Victor Kuncser

This work was supported by the U.S. National Science Foundation under Grant No. 1904714. This research used resources of the Advanced Photon Source, a U.S. Department of Energy (DOE) Office of Science User Facility, operated for the DOE Office of Science by Argonne National Laboratory under Contract No. DE-AC02-06CH11357.

✉ S. H. Lohaus
slohaus@caltech.edu

B. Fultz
btf@caltech.edu

[1] Jet Propulsion Laboratory, 4800 Oak Grove Drive, Pasadena, CA 91109 USA

[2] Department of Applied Physics and Materials Science, California Institute of Technology, Pasadena, CA 91125, USA

1 Introduction

Fundamentally, the free energy of a material originates with its atom configurations, atom vibrations (phonons), and electrons and spins (magnons). The contribution from phonons usually dominates, and can be determined from phonon density of states (DOS) [1]. At a more fundamental level, we seek to understand the energies of phonons in terms of the electron spins and the electronic structure.

Magnons are quanta of spin excitations, typically described as waves of spins in a crystal. Magnons are often described in the low-temperature limit of ferromagnets with localized spins, where they are treated as independent excitations. In the Bloch analysis, the number of magnons increases as $T^{3/2}$, and at modest temperatures (typically above some tens of K), the energy to create another magnon depends on the number of magnons already present. This many-body aspect of magnons has similarities to interactions between phonons in anharmonic potentials, but many-body effects are arguably stronger for magnons. The concept of an individual magnon therefore becomes less useful at room temperature.

Temperature brings more interactions between phonons, as well as between magnons. Furthermore, the atomic displacements of phonons alter the exchange interactions between spins, and vice-versa. This gives "magnon-phonon" interactions that are the subject of our present paper. Our window is through the phonons, which are studied by nuclear resonant inelastic x-ray scattering (NRIXS) measurements of the partial phonon density of states (DOS) of ^{57}Fe atoms [2]. Phonons dominate the entropy of materials at temperatures of a few hundred K. At a temperature of 1000 K, the phonons typically account for an entropy of order 10 k_B/atom (about 7 k_B/atom for both bcc iron and cementite [3]), whereas the entropy contributions from electrons, magnons, and chemical disorder are smaller by an order of magnitude. For thermodynamics it is important to know all these contributions, but small fractional changes in phonon frequencies can make a large contribution to the phonon entropy and free energy of a material.

In the following, we present experimental evidence for thermodynamically-significant effects of the coupling between phonons and magnetism. As a framework for interpreting the effect of magnetization M on the phonon frequencies, we develop a magnetic quasiharmonic approximation, in analogy to the QHA for phonons. Experimental results from nuclear resonant inelastic x-ray scattering (NRIXS) and nuclear forward scattering (NFS) of synchrotron radiation show that the magnetic QHA is useful for demonstrating the importance of magnon-phonon interactions, but it does not identify the origin of these interactions.

2 Experimental Methods and Results

All experimental data were acquired by nuclear resonant inelastic x-ray scattering (NRIXS) and nuclear forward scattering (NFS) at the Advanced Photon Source (APS) at beamline 16ID-D. Essential results were published in [4, 5] and in the Ph.D. thesis by one of the authors [3]. Iron foils with 95% ^{57}Fe isotopic enrichment and 25 μm in thickness were used for the experiments. Cementite was prepared by placing 95% isotopically enriched ^{57}Fe powder and graphite powder inside a volume press at 1 GPa and 1373 K for 102 h. High-temperature experiments used a radiative heating furnace described in [4], and NRIXS measurements performed below room temperature employed a He flow Be-dome cryostat.

Figure 1a shows some of the NRIXS spectra [3] of bcc ^{57}Fe from 30 K through 1185 K, and Fig. 1b shows the phonon DOS obtained from them after using the PHOENIX software

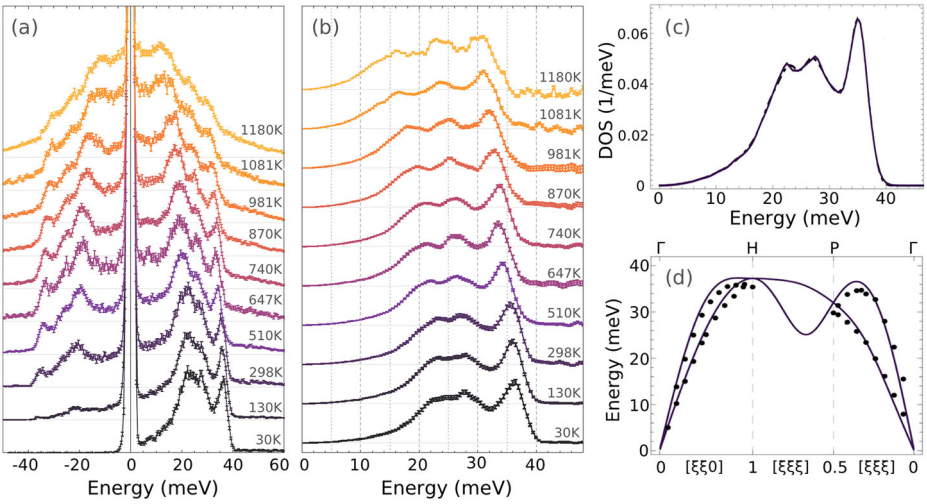

Fig. 1 **a** NRIXS spectra of bcc ^{57}Fe at temperatures from 30 K to 1180 K. **b** Phonon DOS of bcc ^{57}Fe from spectra of panel a. **c** Comparison of fit with the Born-von Kármán model (dashed line) to the phonon DOS at 298 K. **d** Comparison of phonon dispersions from Born-von Kármán model fit at 298 K with the 295 K neutron triple-axis measurements [4]

package for analysis of thermal effects such as multiphonon scattering [6]. A global minimizer was used to fit the phonon DOS curves to predictions of a Born-von Kármán model [3] (Fig. 1c), from which phonon dispersion curves were obtained as in Fig. 1d.

All phonon modes of iron shifted to lower energies with increasing temperature. The essential behavior of the phonon modes was determined by fitting three Lorentzians to the three main peaks of the phonon DOS (the three peaks are those seen in Fig. 1c). Figure 2a shows that the frequencies of the low transverse phonons changed the most above 700 K. The dashed lines of Fig. 2 are predictions of the QHA model for phonons, which fails to track the energy shifts above 600 K. As shown later in Fig. 5, the deviations from the QHA in Fig. 2 follow the change in magnetization of iron with temperature, $M(T)$. In contrast, many-body theory for 3- and 4-phonon processes predicts thermal shifts of phonon energies that are linear in T [7, 8].

Partial phonon densities of states (pDOS) of ^{57}Fe in cementite, $^{57}Fe_3C$, were obtained from cryogenic temperatures through the Curie transition at 460 K using NRIXS [5]. The low temperature pDOS at 14 K is compared to the one at 463 K in Fig. 3. The frequencies of a few phonon branches, notably the acoustic modes of energies below 12 meV, increased with temperature (as shown in insert of Fig. 3). The energies of most phonons decreased with temperature, however. The resulting overall mean phonon energy of cementite remains largely constant with temperature below T_C, as shown in Fig. 2b. This behavior is not captured by the QHA, which predicts a stronger decrease of phonon frequencies. The deviation from the QHA is much smaller than for iron, but the deviation is again approximately proportional to the loss of magnetization with temperature. At higher temperatures, the mean phonon energy decreases rapidly, as shown by both the measurements and the QHA.

The evolution of the magnetic state of $^{57}Fe_3C$ with temperature was measured by nuclear forward scattering (NFS), as shown in Fig. 4. We fitted the data in this work using CONUSS [9] to two Gaussian magnetic hyperfine field distributions, corresponding to the two distinct iron sites in the Fe_3C crystal. At room temperature we find a mean hyperfine magnetic field

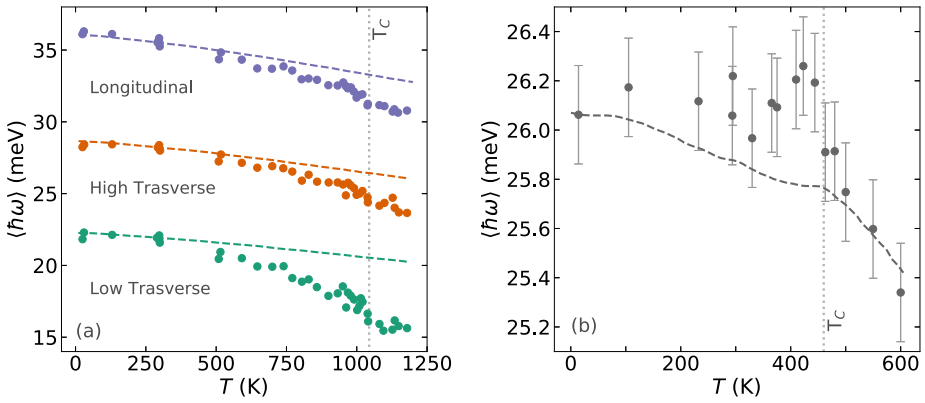

Fig. 2 Mean phonon energies $\langle\hbar\omega\rangle$ measured by NRIXS as functions of temperature for **a** the three phonon modes of Fe and **b** Fe_3C. The phonon energies are compared to the QHA prediction from low temperature measurements (dashed lines). The Curie temperatures at 1044 K and 460 K are marked by vertical lines

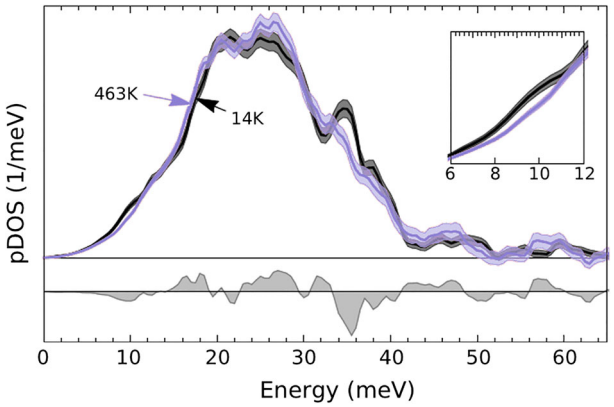

Fig. 3 Partial phonon densities of states (pDOS) of ^{57}Fe in $^{57}Fe_3C$ obtained through NRIXS at 14 K and 463 K. [5]

of $B_{hf} = 20.8$ T, in good agreement with [10] and [11]. The magnetic beats of the NFS spectra of Fig. 4a are suppressed with increasing temperature and disappear at a Curie temperature, T_C of 460 K, in agreement with [12] and about 20 K lower than [10]. The fitted mean B_{hf} below the Curie transition are presented in Fig. 4b, together with data from the literature.

3 Discussion

3.1 Standard phonon quasiharmonic approximation

The phonon free energy for a three-dimensional material with N atoms is [1]

$$F(T) = \int_0^\infty \frac{\hbar\omega}{2} 3Ng(\omega)\,\mathrm{d}\omega + k_B T \int_0^\infty \ln\left(1 - \mathrm{e}^{-\frac{\hbar\omega}{k_B T}}\right) 3Ng(\omega)\,\mathrm{d}\omega\,, \tag{1}$$

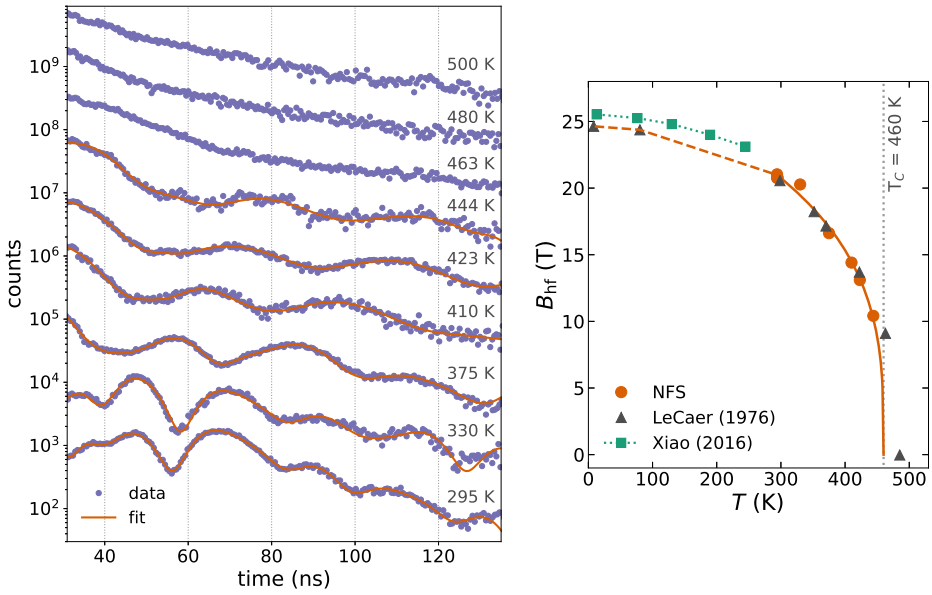

Fig. 4 **a** Nuclear forward scattering (NFS) spectra of Fe_3C at several temperatures. The spectra were fitted using CONUSS, displayed on a log scale, and are offset for clarity. **b** Mean hyperfine magnetic fields B_{hf}, from fitted NFS curves of panel a compared to measurements by Le Caër, et al. [10], and Xiao, et al. [11]. Solid orange curve is a power law fit, and dashed orange curve is the extrapolation to low temperatures using [10]

where the phonon density of states (DOS), $g(\omega)$, is normalized to 1. This simplifies in the high T limit to

$$F_0(T) = 3Nk_BT \int_0^\infty \ln\left(\frac{\hbar\omega}{k_BT}\right) g(\omega)\, d\omega\,. \tag{2}$$

For a harmonic solid, $g(\omega)$ is independent of temperature. This harmonic approximation may account for most of the phonon free energy, but phenomena like thermal expansion cannot be predicted unless the phonon frequencies change with temperature.

As a next step, a Grüneisen parameter γ_i accounts for the fractional change in frequency of mode i per fractional change in volume V

$$\gamma_i = -\frac{V_0}{\omega_i}\frac{\partial\omega_i}{\partial V}\,, \tag{3}$$

where V_0 is an initial volume. The $\{\gamma_i\}$ specify the volume dependencies of the individual mode frequencies $\{\omega_i\}$. Here we simplify by using an average γ for all modes

$$\omega(V_0 + \Delta V) = \omega_0\,(1 - \gamma\,\Delta V/V_0)\,. \tag{4}$$

Using this $\omega(V)$ in (1) or (2) gives a "quasiharmonic approximation" (QHA) for the free energy. In the QHA, the phonons are still non-interacting, but their frequencies shift with volume. Thermal expansion is efficiently predicted with methods of density functional theory that implement the QHA [13]. The reliability of the QHA is uncertain because with true anharmonicity, phonon frequencies have an explicit dependence on T and V as $\omega(V, T)$

[7, 8, 14], which differs from the $\omega(V(T))$ used in the QHA [15, 16]. To develop the QHA from (2), we expand the log functions

$$F(T) = 3Nk_BT \int_0^\infty \ln\left(\frac{\hbar\omega_0\,(1-\gamma\,\Delta V/V_0)}{k_BT}\right) g(\omega)\,d\omega\,, \tag{5}$$

$$F(T) = F_0(T) - 3Nk_BT \int_0^\infty \gamma\,\Delta V/V_0\, g(\omega)\,d\omega\,, \tag{6}$$

$$F(T) = F_0(T) - 3N\gamma k_BT\,\Delta V/V_0\,, \tag{7}$$

where $F_0(T)$ is given by (2) and the last line used the normalization of $g(\omega)$.

With a volume coefficient of thermal expansion β and a change of temperature ΔT, the crystal expands by the amount $\Delta V = \beta\Delta T V_0$. For thermal expansion, the total free energy will include an elastic energy

$$F(T+\Delta T) = F_0(T) - 3Nk_BT\gamma\,\beta\,\Delta T + \frac{1}{2}B\,(\beta\,\Delta T V_0)^2\,, \tag{8}$$

where B is the bulk modulus. In a typical case with $\gamma \simeq +2$, F is reduced by expanding the crystal as the decreasing phonon free energy competes with the increasing elastic energy. Minimizing (8) gives an equilibrium value of thermal expansion $\beta = \gamma 3Nk_B/B$. With $c_V = 3Nk_B$/atom in the classical limit, we obtain the widely-stated result

$$\beta = \frac{\gamma c_V}{B}\,. \tag{9}$$

Equation (9) has been used to define a "magnetic Grüneisen parameter" when β and c_V are attributed to magnetism (early examples are [17, 18]).

3.2 Magnetic quasiharmonic approximation

Following a parallel development, consider a new magnetic Grüneisen parameter based on phonons, γ_m, that is the fractional change in frequency per fractional change in magnetization, M,

$$\gamma_m = +\frac{M_0}{\omega_0}\frac{\partial\omega}{\partial M}\,, \tag{10}$$

which can be compared to (3). This gives a magnetization dependence to ω

$$\omega(M_0+\Delta M) = \omega_0\,(1+\gamma_m\,\Delta M/M_0)\,. \tag{11}$$

To develop a magnetic QHA for $F(T)$, we need the temperature-dependent magnetization $M(T)$. For ferromagnets the general behavior is well known, and $\partial M/\partial T$ has a negative sign. This $\partial M/\partial T$ is largest near the Curie temperature. Using $\omega(M)$ of (11) in (1) or (2), and following the analysis of the previous section for the QHA

$$F(M_0+\Delta M) = F(M_0) + 3N\gamma_m k_BT\,\Delta M/M_0\,. \tag{12}$$

For a change in temperature of ΔT

$$F(T+\Delta T) = F_0(T) + 3N\gamma_m k_BT\,\frac{1}{M_0}\frac{\partial M}{\partial T}\Delta T\,. \tag{13}$$

If γ_m is independent of temperature as we assume, (13) can be integrated from $T' = 0$ to $T' = T$

$$F(T) = F_0(T) + 3N\gamma_m k_BT\,\frac{M(T)-M_0}{M_0}\,, \tag{14}$$

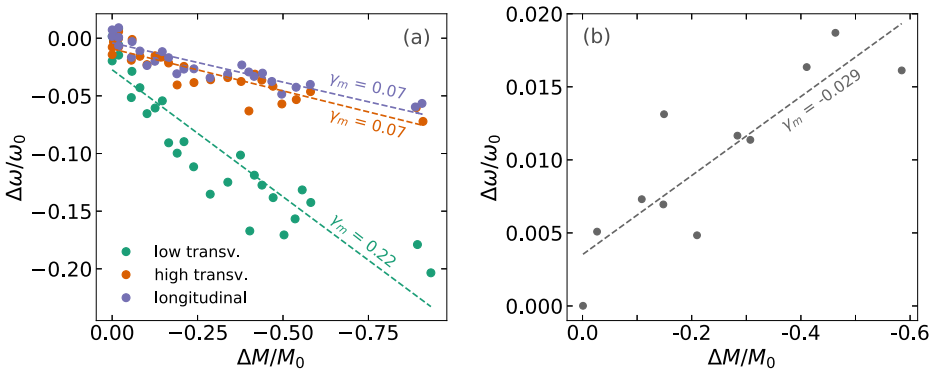

Fig. 5 Fractional deviation of the phonon energy from the QHA ($\Delta\omega/\omega_0$) vs. fractional change of the magnetization ($\Delta M/M_0$) for (a) Fe and (b) Fe_3C. Magnetization data for Fe are from [19]. Dashed lines and labeled values are results of linear fits to the data, corresponding to magnetic Grüneisen parameters γ_m of (10)

so the interaction term in (14) is zero at $T = 0$, and causes F to decrease until the Curie temperature. (For a more complete free energy, we expect a contribution from magnetic short-range order above the Curie temperature, even though the long-range order is zero).

In the classical limit of this magnetic QHA, the effect of magnetism on the phonon free energy, $F = E - TS$, is entirely from the phonon entropy S. Here the phonon energy E remains as $k_B T$ per mode, and is unchanged by magnetism. These are the same roles played by E and S in the standard QHA, but in the magnetic QHA it is M instead of V that alters the phonon entropy and free energy. Using a free energy composed of phonon entropy plus magnetic energy, it is possible to obtain a result parallel to (9) for $M(T)$ (instead of a $V(T)$). This would miss the key contribution from spin entropy, however, which is central to the thermodynamics of magnetism. Nevertheless, it would point out the importance of phonons to magnetization behavior, such as shifts of $M(T)$ and the Curie temperature. Such effects scale with γ_m and the c_V from phonons.

3.3 Magnetic quasiharmonic approximation for iron and cementite

Changes with temperature of the average magnetization and the average phonon frequency were determined with experimental data from NFS and NRIXS, respectively, using results like those shown in Figs. 2 and 4. Magnetic Grüneisen parameters γ_m are defined with (10), but for γ_m to be useful, it must be largely independent of temperature to near the Curie temperature. Figure 5 shows that this is true for the three iron modes, and also for cementite. The dashed lines are linear fits that give values of γ_m. These correlations between the demagnetization and the shift of phonon energies for both iron and cementite motivate the development of a magnetic QHA, which uses the assumption of a constant γ_m in (14).

To further test the magnetic QHA, magnetic Grüneisen parameters were obtained by fitting (14) to the phonon free energy differences for iron and cementite.[1] Figure 6 shows these fits and the phonon free energy data points from NRIXS data. Magnetization curves

[1] In the classical limit, this phonon free energy difference is simply $-T\,\Delta S$, where ΔS is the difference of the experimental phonon entropy from NRIXS and the quasiharmonic phonon entropy. This ΔS is reported in Refs. [4] and [5].

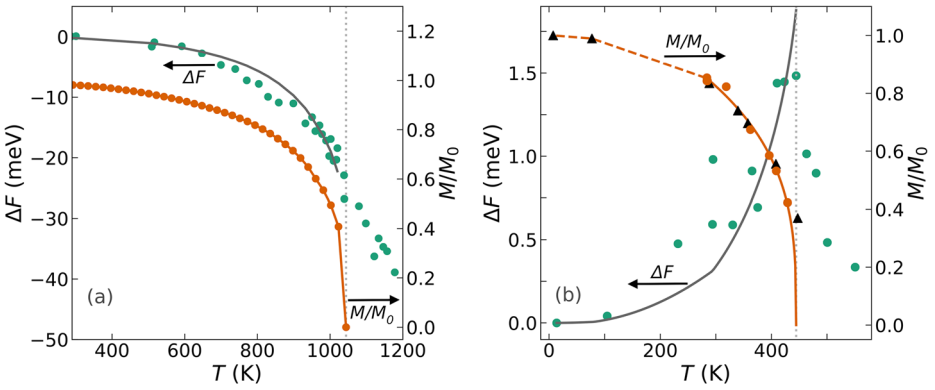

Fig. 6 Deviation of the phonon free energy from the QHA (ΔF, left axes) and evolution of the magnetization (M/M_0, right axes) with temperature for **a** Fe and **b** Fe_3C. Magnetization data for Fe are from [19], and magnetization of Fe_3C is the reduced mean hyperfine magnetic field B_{hf} of Fig. 4. Solid black curves are fits of the magnetic QHA (14) to ΔF from NRIXS data, resulting in $\gamma_{m,\,Fe} = 0.15$ and $\gamma_{m,\,Fe_3C} = -0.028$

Table 1 Grüneisen parameters in the QHA and magnetic QHA

	Standard QHA $V(T), \omega(V), \gamma$	Magnetic QHA $M(T), \omega(M), \gamma_m$	
		Fig. 5 (10)	Fig. 6 (14)
Fe	$\gamma = 2.18$	$\gamma_{m,LT} = 0.22$	$\gamma_m = 0.15$
		$\gamma_{m,\,HT} = 0.07$	
		$\gamma_{m,\,L} = 0.07$	
		$\langle\gamma_m\rangle = 0.13^{(1)}$	
Fe_3C	$\gamma = 2.24$	$\gamma_m = -0.029$	$\gamma_m = -0.028$

The quantities for the standard QHA are from [3]. The magnetic γ_m were determined from fits of the phonon energy shifts with magnetization (Fig. 5, (10)) and from fits of the phonon free to the magnetic QHA (Fig. 6, (14)).
(1) This is the weighted average of the three iron modes in the phonon DOS

are also shown on the same graphs. For iron, the magnetic quasiharmonic model generally captures the behavior of the free energy and its temperature dependence is proportional to $T(M(T) - M_0)$, as predicted by (14). The fit is less reliable for cementite because the difference between the phonon free energy from QHA calculations and NRIXS measurements (ΔF) is small and hard to measure (see scatter in Figs. 2b and 6b). Nevertheless, cementite shows a magnetic Grüneisen parameter of the opposite sign than iron, where the measured phonon energies from NRIXS are larger than from QHA predictions. As seen from the fit of Fig. 6b, the behavior of cementite is also captured adequately by the magnetic QHA approximation, using a small and negative value of γ_m.

The values of γ_m determined by fitting the phonon energy shifts with magnetization (Fig. 5), and the γ_m from fitting the phonon free to the magnetic QHA of (14) (Fig. 6) are very similar, both for iron and for cementite. These values are listed in Table 1, along with the standard phonon Grüneisen parameters.

3.4 Origin of magnon-phonon interactions

Why a phonon frequency would depend on magnetization has been a topic of interest for many years. With many-body theory, in 1969 Silberglitt [20] considered the creation of magnons from phonons, and commented that a spin zero phonon would create two magnons of opposite spin, in addition to satisfying kinematical requirements of energy and momentum conservation for the interaction. For band magnetism, in 1989 Kim [21] considered how the electron-phonon interaction involving free electrons would affect magnetism, and vice-versa.

For ferromagnetic iron, the band structure is polarized, with more electrons in the ↑-band than the ↓-band. A transfer of electrons with temperature from the ↑-band to the ↓-band leads to changes in the density of electron states at the Fermi level. Such changes alter the number of electrons that are available to screen the ion displacements in atom vibrations, altering the interatomic forces. Changes of phonon frequencies with electron density at the Fermi level are well-known [1]. A net gain of electron density at the Fermi level can occur as magnetization is lost near the Curie transition of a ferromagnet. In other words, the electron-phonon interaction will tend to reduce phonon frequencies as magnetism is lost, making a positive contribution to the free energy.

The large difference of γ_{m} between iron and cementite is not readily explained with the simple electronic DOS at the Fermi level – the polarized electronic DOS curves are similar for both, and of course the difference in γ_{m} for the different phonon branches in iron cannot be explained with this simple approach. More subtle effects of the magnetization on phonons are needed to explain the difference in the γ_{m} of bcc iron and cementite. Different phonon branches often have very different changes with temperature. In the standard QHA there is a substantial cancellation of phonon effects from the different mode Grüneisen parameters $\{\gamma_i\}$, with their different signs and magnitudes. This may be true for the different phonon responses to magnetism, requiring individual mode magnetic Grüneisen parameters $\{\gamma_{\mathrm{m},i}\}$, too. Finally, from work with mode Grüneisen parameters in non-magnetic materials, it is known that when the γ_i take large values of 10 or so, or have negative signs, the QHA is generally unreliable and many-body theory of anharmonicity is needed for quantitative explanations [1, 15, 16, 22]. Many-body theory may also be necessary for the interactions of phonons with magnetic spins. Nevertheless, the magnetic QHA does predict approximately the shape of the phonon free energy curves beyond the standard QHA for phonons. It is easy to use, and makes a good case that phonons in iron and cementite depart from the standard phonon QHA owing to magnon-phonon interactions.

4 Conclusions

NRIXS measurements show that both bcc iron and cementite have phonon free energies that deviate from the standard QHA for phonons, with deviations being largest near the Curie temperature. In the case of iron this extra free energy makes a substantial contribution to stabilizing the bcc phase near the Curie temperature and slightly above [3]. We propose a magnetic quasiharmonic theory, akin to the QHA for phonons, using a magnetic Grüneisen parameter, γ_{m}, that is the fractional change in phonon frequency per fractional change in magnetization. This formalism predicts a deviation from the QHA in proportion to $T(M(T) - M_0)$. It accounts for the thermal trends of the phonon free energy beyond the QHA for iron and cementite, and it helps to identify the presence of magnon-phonon interactions. In practice, it requires only data from NFS and NRIXS, and a comparison

of their trends. The physical origins of their different γ_m remain a challenge to explain, however.

Acknowledgements For help with the experiments and their analysis, the authors thank our present and former Caltech colleagues P. Guzman, C. Bernal, M. S. Lucas, C. N. Saunders, J. A. Muñoz, S. J. Tracy, M. Kresch, J. E. Herriman and O. Hellman, and our colleagues at the Advanced Photon Source E. E. Alp, W. Sturhahn, Y. Xiao and P. Chow. We thank J. Li, U. Michigan, for providing the sample of $^{57}Fe_3C$.

Declarations

Conflict of Interests The authors declare that they have no conflict of interest.

References

1. Fultz, B.: Phase transitions in materials. Cambridge Univ. Press, Cambrige (2020)
2. Toellner, T.S., Hu, M.Y., Sturhahn, W., Quast, K., Alp, E.E.: Inelastic nuclear resonant scattering with sub-meV energy resolution. Appl. Phys. Lett. **71**, 2112 (1997). https://doi.org/10.1063/1.120448
3. Mauger, L.: The phonon thermodynamics of iron and cementite. Dissertation (Ph.D.) California Institute of Technology (2015). https://doi.org/10.7907/Z9TQ5ZH3
4. Mauger, L., Lucas, M.S., Muñoz, J.A., Tracy, S.J., Kresch, M., Xiao, Y., Chow, P., Fultz, B.: Non-harmonic phonons in α-iron at high temperatures. Phys. Rev. B **90**, 064303 (2014). https://doi.org/10.1103/PhysRevB.90.064303
5. Mauger, L., Herriman, J.E., Hellman, O., Tracy, S.J., Lucas, M.S., Muñoz, J.A., Xiao, Y., Li, J., Fultz, B.: Phonons and elasticity of cementite through the Curie temperature. Phys. Rev. B **95**, 024308 (2017). https://doi.org/10.1103/PhysRevB.95.024308
6. Sturhahn, W. https://www.nrixs.com/products.html
7. Maradudin, A.A., Fein, A.E.: Scattering of Neutrons by an Anharmonic Crystal. Phys. Rev. **128**, 2589 (1962). https://doi.org/10.1103/PhysRev.128.2589
8. Wallace, D.C. Thermodynamics of Crystals (Dover, 1998) Chap. 18
9. Sturhahn, W.: CONUSS and PHOENIX: Evaluation of nuclear resonant scattering data. Hyperfine Interact. **125**, 149–172 (2000). https://doi.org/10.1023/A:1012681503686
10. Le Caer, G., Dubois, J.M., Senateur, J.P.: Etude par spectrométrie Mössbauer des carbures de Fer Fe3C et Fe5C2. J. Solid State Chem. **19**, 19–28 (1976). https://doi.org/10.1016/0022-4596(76)90145-6
11. Liu, X.-W., Zhao, S., Meng, Y., Peng, Q., Dearden, A.K., Huo, C.-F., Yang, Y., Li, Y.-W., Wen, X.-D.: Mössbauer spectroscopy of iron carbides: from prediction to experimental confirmation. Sci. Rep. **6** (2016). https://doi.org/10.1038/srep26184
12. Bhadeshia, H.K.D.H.: Cementite. Int. Mater. Rev. **65:1**, 1–27 (2020). https://doi.org/10.1080/09506608.2018.1560984
13. Togo, A., Tanaka, I.: First principles phonon calculations in materials science. Scripta Mat. **108**, 1–5 (2015). https://doi.org/10.1016/j.scriptamat.2015.07.021
14. Hellman, O., Abrikosov, I.A., Simak, S.I.: Lattice dynamics of anharmonic solids from first principles. Phys. Rev. B **84**, 180301 (2011). https://doi.org/10.1103/PhysRevB.84.180301
15. Shen, Y., Saunders, C.N., Bernal, C.M., Abernathy, D.L., Manley, M.E., Fultz, B.: Anharmonic origin of the giant thermal expansion of NaBr. Phys. Rev. Lett. **125**, 085504 (2020). https://doi.org/10.1103/PhysRevLett.125.085504
16. Kim, D.S., Hellman, O., Herriman, J., Smith, H.L., Lin, J.Y.Y., Shulumba, N., Niedziela, J.L., Li, C.W., Abernathy, D.L., Fultz, B.: Nuclear quantum effect with pure anharmonicity and the anomalous thermal expansion of silicon. Proc. Nat'l Acad. Sciences **115**, 1992 (2018). https://doi.org/10.1073/pnas.1707745115
17. Simpson, M.A., Smith, T.F.: Magnetic Gruneisen parameters of the Kondo systems CuFe, CuCr, and MoFe. J. Phys. F:, Met. Phys. **11**, 397 (1981). https://doi.org/10.1088/0305-4608/11/2/012
18. Fawcett, E.: Magnetic Gruneisen parameters in chromium. J. Phys.: Condens. Matter **1**, 203 (1989). https://doi.org/10.1088/0953-8984/1/1/017
19. Crangle, J., Goodman, G.M.: The magnetization of pure iron and nickel. Proc. Roy. Soc. Lond. A **321**, 477–491 (1971). https://doi.org/10.1098/rspa.1971.0044

20. Silberglitt, R.: Effect of spin waves on the phonon energy spectrum of a Heisenberg Ferromagnet. Phys. Rev. **188**, 786 (1969). https://doi.org/10.1103/PhysRev.188.786
21. Kim, D.J.: The electron-phonon interaction and itinerant electron magnetism. Phys. Rep. **171**, 129–229 (1989). https://doi.org/10.1016/0370-1573(88)90001-4
22. Li, C.W., Tang, X., Muñoz, J.A., Keith, J.B., Tracy, S.J., Abernathy, D.L., Fultz, B.: Structural relationship between negative thermal expansion and quartic anharmonicity of cubic. Phys. Rev. Lett. **107**, 195504 (2011). https://doi.org/10.1103/PhysRevLett.107.195504